Solid-State NMR Studies of Lead-Containing Zeolites

Heiko G. Niessen,[†] Michelle Van Buskirk, Cecil Dybowski,[‡] David R. Corbin,[§] Jeffrey A. Reimer,* and Alexis T. Bell

Department of Chemical Engineering, 201 Gilman Hall, University of California, Berkeley, Berkeley, California 94720-1462

Received: September 21, 2000; In Final Form: January 25, 2001

We describe ^{207}Pb NMR spectra and ^{27}Al−^{207}Pb double resonance data that derive from a series of lead-containing zeolites. We propose that lead cations are strongly affected by the sorption of water, with the NMR spectra of the resulting material consistent with a chemical equilibrium between Pb^{2+} cations and $PbOH^{+}$ cations. Double resonance experiments on dehydrated samples yield Pb−Al distances consistent with reported X-ray structure.

I. Introduction

A growing body of literature has shown that metal cations exchanged into zeolites can catalyze a wide variety of chemical reactions in a manner similar to organometallic complexes.[1−3] When metal cations are charge exchanged into a zeolite, the zeolite framework acts as the ligand and affects the electronic and hence catalytic properties of the cation. The geometry and composition of the zeolite framework, as well as the presence or absence of framework defects, can also affect the catalytic activity of the cations. Since the size of the pores in zeolites can be similar to those of reactants and products, geometric constraints imposed by carrying out reactions within zeolites can afford additional advantages. Exchange of transition metal cations (e.g., Cu^{+}, Fe^{3+}, Zn^{2+}) into zeolites produces catalysts that are of potential utility for both chemical synthesis and the destruction of gaseous pollutants (e.g., NO and N_2O).[3−5] While much is known about acidic and basic zeolites, the properties and catalytic performance of metal-cation-exchanged zeolites are not well understood. Important issues that need to be addressed include the determination of the stability of transition metal cations to migration in the presence of water and the identification of the location of transition metal cations relative to the zeolite framework.

The interaction of sorbates with ions in zeolites has been addressed theoretically and experimentally.[6] Binding sites near ions have been found through molecular dynamics simulations or quantum chemical calculations for specific structures, but the possibility of changes in structure and dynamics of the framework and ions is often restricted in such calculations. The influence of interactions between ions and organic sorbates on structure and dynamics can also be addressed by spectroscopic techniques. NMR spectroscopy of nuclei in the sorbed molecules has been particularly successful at demonstrating the mobility of molecules and the type of sites at which they are bound.[7,8] To a lesser extent, NMR spectroscopy of ions has been used to probe the local ionic environment.[9,10] In this paper, we report ^{207}Pb and ^{27}Al−^{207}Pb double resonance NMR data that probe the location of the Pb cations in A, X, and Y zeolites and their mobility upon exposure to water. A quantitative model for the interaction of Pb with water is suggested that includes a chemical equilibrium between two forms of the Pb cations.

TABLE 1: Elemental Constitution of the Zeolites

zeolite	Pb unit cell	Si unit cell	Al unit cell	Na unit cell	Si Al	Pb Al
Pb−A[a]	6.1	11.5	12.5		0.92	0.49
Pb−X	44.4	104.0	88.0	0.5	1.18	0.50
Pb−Y	25.6	134.0	58.0	2.6	2.31	0.44

[a] Numbers are for the Pb−A pseudocell.

II. Experimental Section

Lead-containing zeolites were obtained by repeated exchange of commercially available zeolites with aqueous lead nitrate, followed by drying and rinsing with excess water. Elemental analysis (via ICP, Table 1) shows that this procedure produces relatively high exchange levels. In addition, we measured silicon-to-aluminum ratios, and these are also reported in Table 1.

NMR samples were prepared by dehydration at 400 °C under flowing dry nitrogen for a period of 2 h, after which they were transferred to an NMR tube in a controlled atmosphere, usually a mixture of dry nitrogen and oxygen. For experiments involving titration of the zeolite with water, dehydrated samples were subsequently rehydrated to a given degree by the following procedure: a dehydrated sample was put into a tube fitted with a septum; a well-defined amount of H_2O or D_2O was injected into the titration tube with a syringe; the sample was allowed to sit at 45 °C for 8−10 h, after which it was cooled to room temperature and NMR measurements were made.

All NMR experiments were performed on a home-built NMR spectrometer utilizing a TECMAG Libra system with a nominal ^{207}Pb resonance frequency of 83.397 MHz. The ^{207}Pb $\pi/2$ pulse width was 5−6 μs. Spectra were acquired with a Hahn-echo sequence to avoid acoustic ringing, with typical echo times of 20−40 μs. Shifts are reported relative to tetramethyllead, using the perpendicular component of solid lead nitrate at −3473.6 ppm as a secondary reference. At some choices of spectrometer frequency, a background signal was observed. For all frequen-

[†] Institute of Physical and Theoretical Chemistry, University of Bonn, Wegelerstrasse 12, 53115 Bonn, Germany.
[‡] Department of Chemistry and Biochemistry, University of Delaware, Newark, DE 19716-2522.
[§] Central Research and Development, DuPont Company, Wilmington, DE 19880-0262.

10.1021/jp003418s CCC: $20.00
Published on Web 03/28/2001

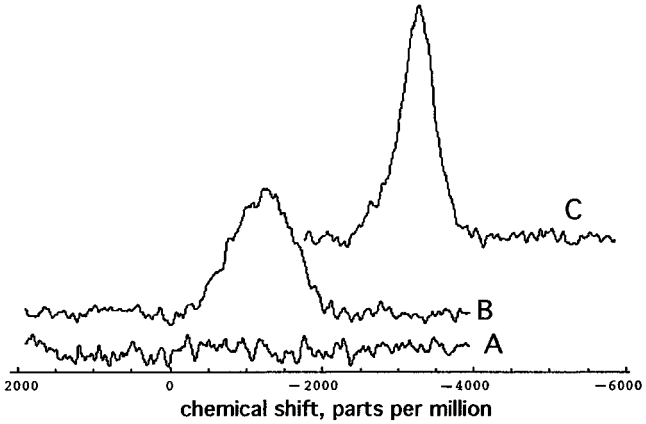

Figure 1. (A) ^{207}Pb NMR spectrum of dehydrated Pb−A zeolite, taken with a relaxation delay of 10 min. (B) ^{207}Pb NMR spectrum of dehydrated Pb−A zeolite, taken with sorption of O_2 gas. (C) ^{207}Pb NMR spectrum of fully hydrated Pb−A zeolite, taken with sorption of O_2 gas.

TABLE 2: NMR Parameters Derived from ^{207}Pb Spectra of O_2 Perfused Zeolites

a. Spin−Lattice Relaxation Times, T_1 (s, ±10%)

sorbates	Pb−A	Pb−X	Pb−Y
O_2	0.83	1.13	1.97
D_2O and O_2	1.1	0.48	1.92
H_2O and O_2	1.13	0.58	2.3

b. Average Shift (ppm, ±10)

sorbates	Pb−A	Pb−X	Pb−Y
O_2	−1100	−1342	−1505
sat'd in D_2O and O_2	−2497	−2749	−2089
sat'd in H_2O and O_2	−2958	−2838	−2275

c. Full Width at Half-Height (kHz, ±2)

sorbates	Pb−A	Pb−X	Pb−Y
O_2	84.9	94.3	-
sat'd in H_2O with O_2	36.7	49.3	33.1

cies used in these experiments, no background signals were observed. We surmise that the background signal emanates from lead-containing solder and that this signal is sufficiently shifted from our detection window to be rendered unobservable under our experimental conditions. Spin−spin relaxation times, T_2, were measured using a Carr−Purcell A sequence with pulse spacings ranging from 60 μs to 1 ms. SEDOR experiments utilized a probe doubly tuned at the lead frequency and the ^{27}Al frequency of 104.3 MHz. The ^{27}Al $\pi/2$ pulse measured for an aqueous $Al(NO_3)_3$ sample was 7.75 μs. Acceptable signal-to-noise ratios required coaddition of 30 000−40 000 acquisitions, depending on the sample and experiment. Magic angle sample spinning (MAS, 3−4 kHz) was attempted on representative samples; in no case was any significant line-narrowing observed.

III. Results

Table 2 and Figure 1 summarize the ^{207}Pb NMR spectra. In most experiments, a small amount of oxygen was admitted to the NMR tube during glovebox transfer to reduce T_1 of the lead nucleus and thus expedite measurements. No significant effect of oxygen[11,12] on shift was detected within our limits of error, but T_1 was shortened from greater than 1 h to about 1 s, thereby affording more rapid acquisition of NMR spectra. One would expect only a few parts-per-million paramagnetic shift[11,12] as a result of oxygen sorption, which is not resolvable in our experiments.

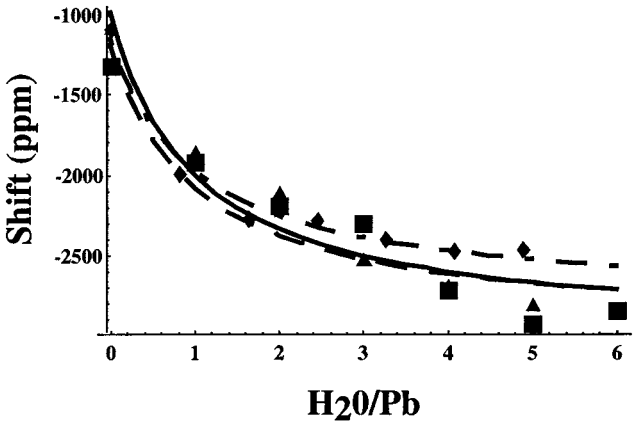

Figure 2. Dependence of average lead chemical shift on H_2O added to a previously dehydrated lead-containing zeolite: Pb−A zeolite (triangles); Pb−X zeolite (squares); Pb−A zeolite as a function of D_2O added (diamonds). Solid lines are fits to the equations given in the text: Pb−A, solid line; Pb−X, dashed line; Pb−A with D_2O, dot−dash line.

The addition of water to a dehydrated zeolite produces changes in intensity, average shift, and width of the lead resonance. A decrease of approximately 40% in the ^{207}Pb signal intensity is observed upon the first dehydration−rehydration cycle. Repeated dehydration−rehydration results in complete loss of observable signal intensity. Elemental analysis confirms, however, that the lead had not been removed from the sample. Addition of either water or D_2O produces (Table 2, Figure 2) a large (negative) shift. Saturation with either water isotope substantially decreases the line width in all three samples.

The dependence of the average lead chemical shift in Pb−A and Pb−X zeolites on the amount of added water has several interesting features. Pb−A and Pb−X have different average shifts in the dehydrated state, but after addition of a single water molecule on average per Pb atom, both Pb−A and Pb−X follow the same dependence on water concentration. (Figure 2) The shift reaches a plateau value with about five to six water molecules added, above which the value remains constant up to saturation. Addition of D_2O to the Pb−A zeolite produces a similar change in shift.

Relaxation and line width data for systematic addition of water and deuterium oxide are shown in Figure 3. Relaxation times follow trends that are virtually identical to the shift data. For both Pb−A and Pb−X, full width at half-height (fwhm) changes in the same manner as the shift, reaching a plateau after five or six water molecules per lead ion are added. The change in fwhm with amount of D_2O added is qualitatively similar.

The pulse sequence for the SEDOR measurement was reported previously.[13,14] Care was taken to ensure that the appropriate length was set for the ^{27}Al π pulse to excite only the central transition, making this a pseudo-spin-1/2 system. The SEDOR fraction $\Delta S(t)$ is defined as the fractional excess signal between a spin echo sequence without an aluminum π pulse applied and one with the π pulse applied:

$$\Delta S(t_1) = \frac{S_o - S_{Al}(t_1)}{S_o} \quad (1)$$

where S_o is the signal amplitude without the aluminum π pulse and $S_{Al}(t_1)$ is the signal amplitude in a sequence with the

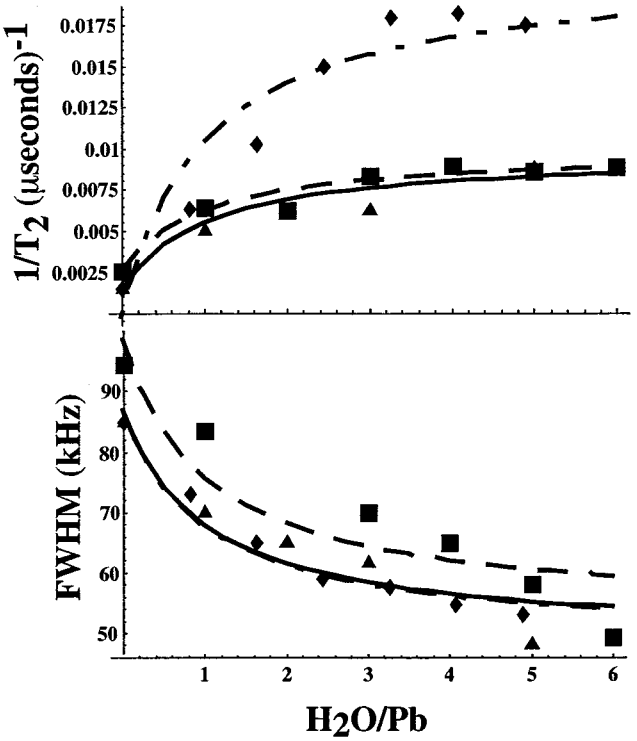

Figure 3. Top: dependence of $1/T_2$, the spin−spin relaxation rate, on H_2O added to a previously dehydrated lead-containing zeolite: Pb−A zeolite (triangles); Pb−X zeolite (squares); Pb−A zeolite as a function of D_2O added (diamonds). Solid lines are fits to the equations given in the text: Pb−A, solid line; Pb−X, dashed line; Pb−A with D_2O, dot−dash line. Bottom: full width at half-height (fwhh) of the ^{207}Pb spectra as a function of added water; symbols are the same as top.

aluminum π pulse applied at t_1. The SEDOR fraction for an isolated spin pair is given as[15]

$$\Delta S(t_1) = 1 - J_o(3\pi D t_1)\cos(\pi D t_1) + 2\sum_{k=1}^{\infty}\frac{1}{4k^2-1}J_k(3\pi D t_1)\cos\left(\pi D t_1 + \frac{k\pi}{2}\right) \quad (2)$$

where D is the dipolar coupling constant:

$$D = \frac{\gamma_{Pb}\gamma_{Al}\hbar}{2\pi r^3} \quad (3)$$

and J_k is a Bessel function. A fit of the variation of $\Delta S(t_1)$ with t_1 gives initial estimates for D, and hence r, for the samples. To refine the estimates, we evaluated χ^2, weighted by the error in the signals, in the vicinity of this value. For weighting factors, we took the estimated noise amplitude as a fraction of the signal amplitude: for Pb−X and Pb−Y, this was 0.15; for Pb−A, it was 0.20. Figure 4 gives the variation of χ^2 as a function of r for Pb−X. A fit of the calculated points to a polynomial allowed us to obtain the minimum and an estimate of the error in this value for each sample. The more typical display of the evaluation of distance in a SEDOR experiment is shown in Figure 5 for the three zeolites. In this figure, data are compared to the best-fit line and two "error estimates" that represent the maximum and minimum acceptable curves through the points. The χ^2 analysis gives a more precise determination of the error, as well as the average value of the internuclear distance assuming an isolated spin pair; using this method, we find the average Pb−Al distances to be 0.235(±0.003), 0.267(±0.004), and 0.262(±0.005) nm for Pb−A, Pb−X, and Pb−Y, respectively.

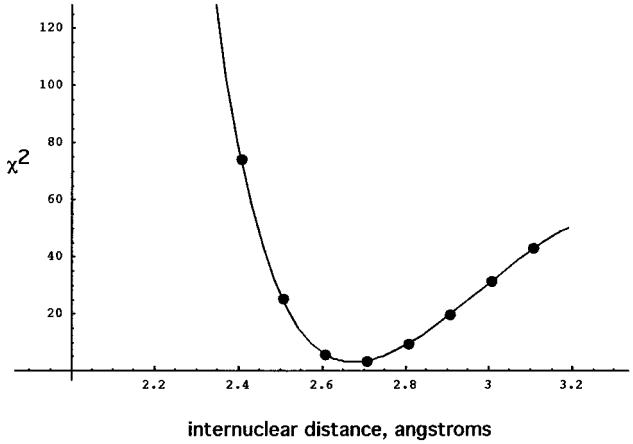

Figure 4. Error χ^2 derived SEDOR equations and experimental data versus Pb−Al internuclear distance r for Pb−X. The solid line shows the polynomial fit to these data, from which the minimum value is found.

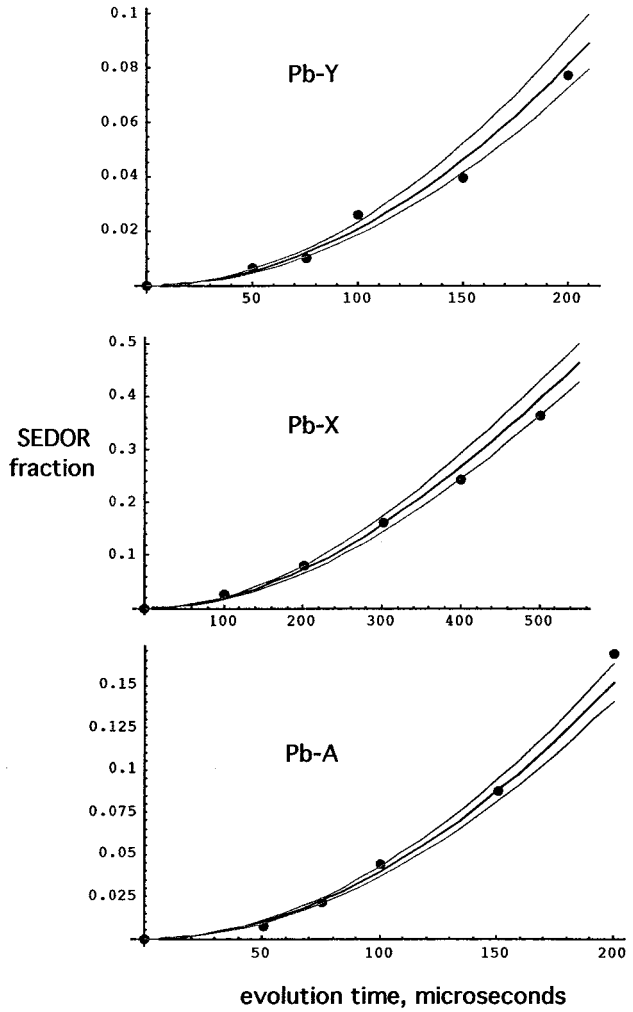

Figure 5. SEDOR data and derived curves for isolated Pb−Al pairs: Pb−Y zeolite (derived internuclear distance is 0.262(±0.005) nm), Pb−X zeolite (derived internuclear distance is 0.267(±0.004) nm), and Pb−A zeolite (derived internuclear distance is 0.235(±0.003) nm).

IV. Discussion

There is no reason to believe that the ^{207}Pb resonances are dominated by anything other than the chemical shift interaction. In the fully hydrated state, the average shifts are comparable to those of lead ions in aqueous solution, for example, lead nitrate solution.[16] In the fully dehydrated state, these average shifts

are consistent with those observed in solids for lead cations surrounded by oxygen-containing anions, such as titanates and zirconates.[17−19] Our data are qualitatively similar to results reported previously for Na,Pb-exchanged Linde A samples.[9] It is not surprising that multiple peaks are not observed for the different cation exchange sites known to exist in these materials. Lithium and sodium shift differences are small,[10,21] and when these values are extrapolated to lead chemical shifts, we find the expected differences to be small compared to the line widths. We surmise, therefore, that the subtle differences in chemical shift between cations associated with the different framework aluminum sites are obscured by significant broadening mechanisms (discussed below).

This is not the case, however, if Pb ions are subject to change in oxidation state. The loss of apparent signal with each dehydration/hydration cycle suggests that, with each hydrothermal treatment, Pb cations are "shuttled" to a chemical environment not detected in our excitation window. If the hydrothermal treatment mediates the production of lead oxides or hydroxy species, one might expect to detect resonances of lead oxides. Recent measurements[17,22,23] indicate that the ^{207}Pb resonances of lead oxides like α-PbO, *β*-PbO, and minium, Pb_3O_4, occur at positive shifts and, given their large spans, would be quite difficult to detect. The shifts of lead in coordination with hydroxy ions are also shifted, with average shifts of ∼−1000 ppm, and also have large spans. Resonances of plumbates tend to fall in this region as well.[24] Previous X-ray studies suggest[20] that Pb may exist in the zeolite in coordination with oxygen (e.g., as PbO_4 moieties). Such species would be expected to have NMR properties similar to the lead oxides and would be very difficult to detect given the narrow (∼2800 ppm) excitation window of our spectrometer.

The full widths at half-maximum (fwhm) of the three dehydrated zeolites are quite large, most likely resulting from dispersion of isotropic lead shifts, chemical-shift anisotropy, relaxation broadening, susceptibility broadening, or some combination of these effects. The fwhms are comparable to chemical-shift anisotropies observed for solid lead materials[17−19,22] and Na,Pb-exchanged Linde A.[9] If we assume that the spectrum shown in Figure 1b represents the powder pattern for a lead at only a single site, we estimate a span, Ω, of approximately 1200 ppm and a skew, *κ*, between 0.0 and 0.2 for this Pb−A site. It is worth noting, however, that anisotropy alone cannot account for the observed line width, as MAS yields no decrease in observed line width.

Addition of water substantially decreases the observed line width. We measured the dependence of T_2 on water content with a Carr−Purcell A sequence (Figure 3, top). Addition of a single water (on average) per Pb atom causes a dramatic drop in T_2; i.e., an efficient lead relaxation mechanism is introduced by the addition of either water or deuterium oxide. Spin−spin relaxation remains relatively constant for higher loadings of water. If relaxation broadening were the major effect, one would expect the fwhm to increase as the first water is added and to remain relatively constant as more water is added. What is observed is the opposite behavior, so we conclude that the variation of fwhm with water content is the result of a narrowing of an inhomogeneous shift distribution as water is added, up to about five or six waters per Pb atom. The limiting value of T_2 (120 *μ*s) corresponds to a contribution to fwhm of ∼2650 Hz (or ∼30 ppm), much less than the observed limiting fwhm.

The systematic changes in relaxation time T_2 and average shift with water content suggest that the chemical environment of the Pb cations is affected by water. We presume that, when hydrated, the lead cation experiences multiply coordinated water molecules and that, when so coordinated, a chemical change in the Pb ion may occur. By analogy with studies of copper cations,[25] we hypothesize that $Pb^{2+}OH^-$ may form in the presence of water. We therefore propose a two-site exchange model consistent with the chemical shift and relaxation time (T_2) data. Consider the following equilibrium reaction:

$$Z_2^-Pb^{2+}\cdot mH_2O \leftrightarrow Z^-[Pb^{2+}OH^-]\cdot(m-1)H_2O + Z^-H^+ \quad (4)$$

For simplicity, we omit the factor m,[26] write $[Pb^{2+}OH^-]$ as $PbOH^+$, and designate the fraction of Pb^{2+} ions as $\Theta_{Pb^{2+}}$; the latter is given by

$$\Theta_{Pb^{2+}} = \frac{n_{Pb^{2+}}}{n_{Pb^{2+}} + n_{PbOH^+}} \quad (5)$$

In the presence of rapid, two-site exchange, the average shift δ is

$$\delta = (\delta_{Pb^{2+}})(\Theta_{Pb^{2+}}) + (\delta_{PbOH^+})(\Theta_{PbOH^+}) = \delta_{Pb^{2+}} + (\Delta_{Pb^{2+},PbOH^+})(\Theta_{PbOH^+}) \quad (6)$$

with

$$\Theta_{Pb^{2+}} + \Theta_{PbOH^+} = 1 \quad (7)$$

The symbol $\Delta_{Pb^{2+},PbOH^+}$ is the shift difference between the Pb^{2+} and $PbOH^+$ sites. It follows that the equilibrium constant **K** can be written in terms of the number f of water molecules admitted per lead ion:

$$f = \frac{n_{H_2O}}{n_{Pb,total}} \quad (8)$$

with $n_{Pb,total}$ is derived from elemental analysis and n_{H_2O} set during sample preparation. We write **K**

$$\mathbf{K} = \frac{\Theta_{PbOH^+}{}^2}{(1-\Theta_{PbOH^+})(f-\Theta_{PbOH^+})} \quad (9)$$

One may solve this expression for Θ_{PbOH^+} and obtain

$$\Theta_{PbOH^+} = -M(1+f) \pm \sqrt{M^2(1+f)^2 + 2Mf} \quad \text{with} \quad M = \frac{\mathbf{K}}{2(1-\mathbf{K})} \quad (10)$$

The observed shifts vary considerably with just a few molecules of water added, and the range of shifts observed ultimately span the range of known shifts for lead hydroxides and solvated lead cations. These observations lead us to suggest that the free energy *difference* between the two lead environments is nearly zero. Thus, we assume that the equilibrium constant **K** is approximately 1, and use a Taylor expansion about $\mathbf{K} = 1$ to simplify (10) to

$$\Theta_{PbOH^+} = \frac{f}{1+f} \quad (11)$$

The total shift is then

$$\delta = \delta_{Pb^{2+}} + (\Delta_{Pb^{2+},PbOH^+})(\Theta_{PbOH^+}) = \delta_{Pb^{2+}} + \mathbf{A}\frac{f}{1+f} \quad (12)$$

The factors $\delta_{Pb^{2+}}$ and **A** may be derived from a nonlinear fit of

TABLE 3: SEDOR Analysis Structural Models

zeolite	Si Al	Pb−Al	Pb−Al_2	Pb−Al_3	X-ray[20]
Pb−A	0.92	0.235	0.296	0.339	0.315−0.358
Pb−X	1.18	0.267	0.336	0.385	
Pb−Y	2.31	0.261	0.329	0.376	

observed shift versus total water added. These fits are shown as lines in Figure 2. The agreement between data and fit is good. The derived parameter **A** from these fits represents the chemical shift difference between the Pb^{2+} and $PbOH^{+}$ environments, and it is determined from water adsorption data to be 1800 ± 200 ppm, almost exactly the same as the isotropic shift difference between aqueous Pb^{2+} cations and PbOHCl.[27]

A similar analysis can be performed for the spin−spin relaxation rate $1/T_2$ (Figure 3, top) and line widths (Figure 3, bottom). The fits are not as compelling as those shown in Figure 2, yet, given the larger uncertainties in the data, we find them to be consistent with the proposed model. The **increased** ^{207}Pb relaxation rate in the presence of deuterium oxide rules out proton/deuteron dipolar relaxation as the main contributor to lead spin−spin relaxation. We surmise that lead motion in the presence of deuterium oxide is different from that for the hydronium oxide, and thus the relaxation data differ. The nature of this motional difference could be related to the different free energies of the hydrated versus deuterated cation, or some other isotope effect. A full suite of temperature and coverage dependent data would be needed to address this question further.

The SEDOR data can provide Pb−Al internuclear distances in the context of a model for the geometric arrangement of the nuclei. The simplest model assumes a single isolated Pb−Al pair. As discussed above, the internuclear distances derived with this model are 0.235 ± 0.003, 0.267 ± 0.0064, and 0.262 ± 0.005 nm for Pb−A, Pb−X, and Pb−Y, respectively. The distance obtained for Pb−A zeolite is shorter than expected, given previous SEDOR measurements of Cu−Al couplings in Cu−ZSM5[14] and the X-ray data for a Pb−A zeolite.[20]

The isolated-pair model, however, is clearly not appropriate for zeolites whose Si/Al ratios are of order unity. The X-ray data[20] published previously for lead-exchanged Pb−A zeolites are more appropriately modeled as Pb cations located within the six-membered rings of the sodalite cages interacting with three aluminum nuclei (where Si/Al = 1) having internuclear distances in the range 0.3145−0.3575 nm. Thus, a better structural model consists of a Pb nucleus at the center of an equilateral triangle of three Al nuclei. Similarly, for zeolites of higher Si/Al ratio, models with a Pb nucleus interacting with two Al nuclei may be appropriate. In these cases, eq 3 may be replaced with a lattice sum over pairwise dipolar interactions. Considering the model of equal distances only, one may use the dipolar frequencies derived from Figure 5 to yield the Pb−Al distances shown in Table 3. From these results, it is seen that the Pb−Al_3 model is consistent with X-ray data for Pb−A, whereas the Pb−Al_2 model provides results consistent with those distances for the Pb−X and Pb−Y samples. Thus, the SEDOR data corroborate a structural model for the Pb sites that is consistent with the X-ray structural studies.

V. Conclusions

The data and analysis reported herein bring together a number of seemingly disparate methods and concepts to yield insight into the siting and hydrothermal stability of metal-exchanged ions in zeolites. First, we note that the use of ^{207}Pb NMR represents an example of emerging *applications* of solid state NMR of less-common nuclei. Indeed, many of our conclusions are justified on the basis of fundamental studies of lead chemical shifts in model compounds. Second, while SEDOR methods are now commonly applied to problems in solid-state chemistry, the present work represents an unusual application of this method to systems other than isolated spin pairs. The corroboration of the X-ray data with the SEDOR model shows how the method may be applied to complex systems. Third, the results of the chemical equilibrium model demonstrate the important role of hydration-sphere chemistry in zeolites to yield complex metal cationic species, such as $M^{2+}OH^{-}$. Fourth, even with little detail of the nature of the hydration chemistry necessary to form $Pb^{2+}OH^{-}$, a two-site exchange model provides semiquantitative fits to the observed experiments, emphasizing the significant role of dynamics in the chemistry of metal-exchanged zeolites. Finally, the loss of observed Pb signal with hydrothermal treatment provides evidence for the "shuttling" of potentially active catalytic cations to sites that are less or differently active.

We conclude that magnetic resonance spectroscopy of metal cations provides a means to assess the siting and hydrothermal stability of metal-exchanged ions in zeolites and may be used further toward an understanding of their unusual catalytic capabilities.

Acknowledgment. J.A.R. and A.T.B. acknowledge support from the National Science Foundation CTS 9713143. C.D. acknowledges support of the donors of the Petroleum Research Fund of the American Chemical Society through Grant 33633-AC5. We acknowledge B. R. Wood for help with dehydration of the zeolites, A. K. Paravastu for discussion of analysis with the program Mathematica, G. Pavlovskaya for pointing out the loss of Pb signal with dehydration/hydartion cycles, and P. Hollins for the preparation of these materials. H.G.N. acknowledges a fellowship of the *Studienstiftung des deutschen Volkes* and the *Dr. Juergen-Ulderup Stiftung* for a special postgraduate research fellowship.

References and Notes

(1) van Bekkum, H., Flanigen, E. M., Jansen, J. C., Eds. Introduction to Zeolite Science and Technology; *Studies in Surface Science and Catalysis*; Elsevier: Amsterdam, 1991; p 58.

(2) Barthomeuf, D. *Catal. Rev.-Sci. Eng.* **1996**, *38*, 521.

(3) Klier, K. *Langmuir* **1988**, *4*, 13.

(4) Armor, J. N. *Science and Technology in Catalysis 1994*; Kondansha: Tokyo, 1995; p 51.

(5) Maxwell, I. E. *Adv. Catal.* **1982**, *31*, 2.

(6) For example, see: (a) Kramer, G. J.; van Santen, R. A.; Emeis, C. A.; Nowak, A. K. *Nature* **1993**, *363*, 529. (b) Rice, M. J.; Chakraborty, A. K.; Bell, A. T. *J. Phys. Chem. A* **1998**, *102*, 7498.

(7) Kustanovich, I.; Luz, Z.; Vega, S.; Vega, A. J. *J. Phys. Chem.* **1990**, *94*, 3138.

(8) Hepp, M. A.; Ramamurthy, V. J.; Corbin, D. R.; Dybowski, C. *J. Phys. Chem.* **1992**, *96*, 2629.

(9) Eldewik, A.; Hook, J. M.; Singh, N. K.; Howe, R. F. *Magn. Reson. Chem.* **1999**, *37*, S63.

(10) (a) Feuerstsein, M.; Lobo, R. F. *Solid State Ionics* **1999**, *118*, 135. (b) Feuerstein, M.; Lobo, R. *Chem. Mater.* **1998**, *10*, 2197. (c) Feuerstein, M.; Engelhardt, G.; Daniel, P. L.; MacDougall, J. E.; Gaffney, T. R. *Micro. Mesopor. Mater.* **1998**, *26*, 27.

(11) Liu, H.; Kao, H−M.; Grey, C. P. *J. Phys. Chem. B* **1999**, *103*, 4786.

(12) Plevert, J.; Menorval, L. C.; Di Renzo, F.; Fajula, F. *J. Phys. Chem. B* **1998**, *102*, 3412.

(13) Kenaston, N. P.; Bell, A. T.; Reimer, J. A. *J. Phys. Chem.* **1994**, *98*, 894.

(14) Hu, S.; Reimer, J. A.; Bell, A. T. *J. Phys. Chem. B* **1997**, *101*, 1869.

(15) Mueller, K. T. *J. Magn. Reson. A* **1995**, *113*, 81.

(16) Altounian, N.; Glatfelter, A.; Bai, S.; Dybowski, C. *J. Phys. Chem. B* **2000**, *104*, 4723.

(17) Neue, G.; Smith, M. L.; Hepp, M.; Perry, D. L.; Dybowski, C. *Solid State Nucl. Magn. Reson.* **1996**, *6*, 241.

(18) Shore, J. S.; Zhao, P.; Prasad, S.; Huang, J.; Fitzgerald, J. J. *J. Phys. Chem. B* **1999**, *103*, 10617.

(19) Fayon, F.; Farnan, I.; Bessada, C.; Coutures, J.; Massiot, D. *J. Am. Chem. Soc.* **1997**, *119*, 6837.

(20) Yeom, Y. H.; Kim, Y.; Seff, K. J. *J. Phys. Chem. B* **1997**, *101*, 5314.

(21) Hunger, M.; Sarv, P.; Samoson, A. *Solid State Nucl. Magn. Reson.* **1997**, *9*, 115.

(22) Gabuda, S.; Kozlova, S. G.; Terskikh, V. V.; Neue, G.; Perry, D. L.; Dybowski, C. *Chem. Phys. Lett.* **1999**, *305*, 353.

(23) Gabuda, S.; Kozlova, S. G.; Terskikh, V. V.; Neue, G.; Perry, D. L.; Dybowski, C. *Solid State Nucl. Magn. Reson.* **1999**, *15*, 103.

(24) Bai, S.; Dybowski, C.; Martinez, D. I.; Segarra, S. O.; Perry, D. L. Unpublished results.

(25) Larsen, S. C.; Aylor, A.; Bell, A. T.; Reimer, J. A. *J. Phys. Chem.* **1994**, *98*, 11533.

(26) The exact nature of charge compensation from the zeolite lattice is not clear, but the model presented here suggests formation of acidic sites with the zeolite.

(27) Smith, M. L.; Hepp, M. A.; Gaffney, E. J.; Neue, G.; Perry, D. L.; Dybowski, C. *Appl. Spectrosc.* **1988**, *52*, 426.